The C-terminal basic residues contribute to the chemical and voltage-dependent activation of TRPA1

Abdul Samad, Lucie Sura, Jan Benedikt, Rudiger Ettrich, Babak Minofar, Jan Teisinger, Viktorie Vlachova

The C-terminal basic residues contribute to the chemical and voltage-dependent activation of TRPA1

Abdul Samad, [1,2,3], Lucie Sura,[1,3], Jan Benedikt,[1], Rudiger Ettrich,[2], Babak Minofar,[2], Jan Teisinger,[1] and Viktorie Vlachova[1*]

[1]*Department of Cellular Neurophysiology, Institute of Physiology, Academy of Sciences of the Czech Republic, Videnska 1083, 142 20 Prague 4, Czech Republic*
[2]*Laboratory of Structural Biology, Institute of Systems Biology and Ecology, ASCR, Zamek 136, 373 33 Nove Hrady, Czech Republic*

[3]*These authors contributed equally to this work*

The ankyrin transient receptor potential channel TRPA1 is a nonselective cationic channel that is expressed by sensory neurons, where it can be activated by pungent chemicals, such as allyl isothiocyanate (AITC), cinnamon or allicin, by deep cooling (< 18°C) or highly depolarizing voltages (> +100 mV). From the cytoplasmic side, this channel can be regulated by negatively charged ligands such as phosphoinositides or inorganic polyphosphates, most likely through an interaction with as yet unidentified positively charged domain(s). In this study, we mutated 27 basic residues all along the C-terminal tail of TRPA1, trying to explore their role in AITC- and voltage-dependent gating. In the proximal part of the C-terminus, the function-affecting mutations were at K969, R975, K988 and K989. A second significant region was found in the predicted helix, centered around K1048 and K1052, in which single alanine mutations completely abolished AITC- and voltage-dependent activation. In the distal portion of the C-terminus, the charge neutralizations K1092A and R1099A reduced the AITC sensitivity, and, in the latter mutant, increased the voltage-induced steady-state responses. Together, our findings identify basic residues in the C-terminus that are strongly involved in TRPA1 voltage and chemical sensitivity, some of them may represent possible interaction sites for negatively charged molecules that are generally considered to modulate TRPA1.

INTRODUCTION

The ankyrin TRPA1 channel is an important constituent of the transduction apparatus through which proalgesic agents, such as allyl isothiocyanate (AITC), various products of oxidative stress, deep cooling or mechanical stimuli depolarize sensory nerve endings to elicit pain. In addition to a range of pungent chemicals that either bind to (cannabinoids, icilin, eugenol, carvacrol, thymol) or covalently interact with TRPA1 (cinnamaldehyde, acrolein), this polymodal nonselective cation channel can also be activated by highly depolarizing voltages (> +100 mV) and calcium ions (Ca^{2+}) that enter through the channel and bind to its N-terminus [1-11]. Depending on the permeating Ca^{2+}, TRPA1 dynamically controls its own

critical properties such as unitary conductance, ion selectivity and open channel probability [12]. An increase in intracellular calcium ($[Ca^{2+}]_i$) not only directly modulates TRPA1 activity but also recruits cellular, Ca^{2+}-dependent signaling cascades which further regulate the channel. Of these, the activation of phospholipase C (PLC) resulting in a decrease in the membrane phosphatidylinositol-4,5-bisphosphate (PIP_2) is of particular interest, because this signaling lipid may act as an important physiological regulator of TRPA1 in sensory neurons [8,13,14].

The negatively charged ligands, such as phosphoinositides or inorganic polyphosphates, regulate TRPA1 from the cytoplasmic side [9,12,15-20], most likely through an interaction with as yet unidentified positively charged domain(s). Based on their analogy to voltage-gated potassium channels (KCNQ, K_{ir}) and various ion channels of the TRP family (TRPV1, TRPM4, TRPM8), the favorite candidates for the interaction of the TRPA1 channel with negatively charged molecules are the membrane-proximal clusters of positively charged residues on the cytoplasmic C-termini, near to but also further away from the sixth transmembrane domain (for reviews, see [15,21,22]). Such a polybasic region may be able to specifically recognize negatively charged phospholipids, but might also act as a sensor for changes in transmembrane voltage. TRPA1 is a voltage-gated ion channel with an estimated apparent number of gating charges of around 0.4 [23]. Compared to voltage-gated potassium channels, the voltage-dependence of TRPA1 is very weak and its putative voltage-sensing domain most likely lies outside the conventionally considered fourth transmembrane segment (S4) because it does not contain any charged residues at all. Thus, in addition to the PIP_2 - interacting domain(s), the location of the voltage-sensing domain also remains enigmatic and awaits determination.

In this study, we set out to screen for sites that have the highest probability of being involved in the above processes. We individually altered the charge character of 27 basic residues all along the C-terminal tail of human TRPA1 and examined the membrane current responses to voltage, AITC, and their combination. We have identified several significant regions within the C-terminus in which positively charged amino acids confer both chemical and voltage sensitivity to TRPA1 channels.

MATERIALS AND METHODS

Expression and Constructs of hTRPA1 channel

HEK293T cells were cultured in OPTI-MEM I medium (Life Technologies) supplemented with 5% FBS as described previously [24,25]. Cells were transiently co-transfected with 300-400 ng of cDNA plasmid encoding wild-type or mutant human TRPA1 (wild type in the pCMV6-XL4 vector, OriGene) and with 300 ng of GFP plasmid (TaKaRa) per 1.6-mm dish using the Magnet-assisted Transfection (IBA GmbH) method. Cells were used 24-48 h after transfection. At least two independent transfections were used for each experimental group. The wild-type channel was regularly tested in the same batch as the mutants. The mutants were generated by PCR using the QuikChange XL Site-Directed Mutagenesis Kit (Stratagene) and confirmed by DNA sequencing (ABI PRISM 3100, Applied Biosystems).

Electrophysiology

Whole-cell membrane currents were recorded by employing an Axopatch 200B amplifier and pCLAMP 10 software (Molecular Devices). Patch electrodes were pulled from a glass tube with a 1.65 mm outer diameter. The tip of the pipette was heat-polished and its resistance was 3-5 MΩ. Series resistance was compensated by at least 70% in all recordings. Experiments were performed at room temperature (23-25°C). Only one recording was performed on any one coverslip of cells to ensure that recordings were made from cells not previously exposed to chemical stimuli. Voltage-dependent gating parameters were estimated from steady-state current-voltage (*I-V*) relationships obtained at the end of 60 or 100-ms voltage steps by fitting the conductance $G = I/(V - V_{rev})$ as a function of the test potential V to the Boltzmann equation: $G = [(G_{max}-G_{min})/(1+\exp(-zF(V - V_{1/2})/RT))] + G_{min}$; where z is the apparent number of gating charges, $V_{1/2}$ is the half-activation voltage, G_{min} and G_{max} are the minimum and maximum whole-cell conductance, V_{rev} is the reversal potential, and F, R, and T have their usual thermodynamic meaning.

A system for rapid superfusion of the cultured cells was used for drug application [26]. The extracellular control solution contained (mM): 160 NaCl, 2.5 KCl; 1 $CaCl_2$, 2 $MgCl_2$, 10 HEPES, 10 glucose; adjusted to pH 7.3 and 320 mOsm. In whole-cell patch clamp experiments, the pipette solution contained (mM): 125 Cs-gluconate, 15 CsCl, 5 EGTA, 10 HEPES, 0.5 $CaCl_2$, 2 MgATP; pH 7.3, 286 mOsm. AITC solution was prepared from a 0.01 M stock solution in water stored at -20 °C. All chemicals were purchased from Sigma-Aldrich.

Statistical analysis

All data was analyzed using pCLAMP 10 (Molecular Devices), and curve fitting and statistical analyses were done in SigmaPlot 10 (Systat Software). Statistical significance was determined by Student's *t*-test or the analysis of variance; differences were considered significant at $P < 0.05$, if not stated otherwise. For statistical analysis of amplitude data a logarithmic transformation was used to achieve normal distribution. Conductance-voltage (*G-V*) relationships were obtained from steady-state whole-cell currents measured at the end of voltage steps from -80 to +200 mV in increments of +20 mV. All data is presented as mean ± SEM.

RESULTS

Mutations within the C-terminal region identified the residues involved in AITC-induced activation of TRPA1

We individually neutralized all 27 positively charged amino acid residues within the C-terminus of human TRPA1 and characterized the phenotypes of mutants using whole-cell patch-clamp recordings from transiently transfected HEK293T cells. The primary and putative secondary structure of this region and the residues chosen for mutagenesis are depicted in Figure 1. The C-terminus was predicted to contain two long (H1: I964-K989, H4:

L1040-K1071) and four short α-helices (H2: W993-V998, H3: L1016-F1022, H5: D1089-Q1095, H6: W1103-K1111). We have previously reported that mutations in the predicted inner vestibule of the TRPA1 channel had strong effects on several aspects of channel functioning, including changes in the voltage-dependent activation/deactivation kinetics and a significant increase in the current variance at depolarizing potentials [27]. We then proposed that the pore-forming S6 helix of TRPA1 may extend to the cytoplasmic region so that the proximal portion of the C-terminus, putatively located near the inner mouth of the pore, might directly participate in the regulation of the channel gating or permeation properties. To consider this issue further, we also introduced mutations other than alanine at the most proximal residues: K969E, K969I, K969R, R975E, R975W, K989N, and K989E.

The functionality of all mutants was initially established by recording whole-cell currents at a holding potential of –70 mV in response to a supersaturating concentration of allyl isothiocyanate (AITC; 200 μM), applied for 20-30 s in the presence of extracellular Ca^{2+} (1 mM), and by measuring the amplitudes of the currents at the peak (Figure 2A). The period of exposure to AITC was prolonged in those constructs that exhibited slower or incomplete activation kinetics (Figure 2Ba-m). As previously described [1,7,9], the AITC-induced responses mediated through wild-type TRPA1 channels were multiphasic with an initial gradually increasing phase followed by a steeper (Ca^{2+} dependent) secondary phase that occurred 10-20 seconds after AITC was applied to the cell for the first time. The steep secondary phase of activation was typically followed by an apparent decline in maximal current amplitude ($T_{50} \sim 18$ s), elsewhere referred to as channel inactivation [9,10]. Despite a high degree of cell-to-cell variability in TRPA1 expression and in the magnitudes of AITC-evoked currents within each experimental group, we were able to detect a statistically significant reduction in responsiveness to AITC in ten alanine mutants ($P < 0.01$; Figure 2C). Three mutation-affected residues were located in the predicted region of the proximal long canonical α-helix H1: K969, R975A and K989. Four residues, K1046, K1048, K1052 and K1071, were identified within the range of the helix H4 (Figure 1). Mutations K1048A and K1052A did not produce measurable currents in response to AITC at a holding potential of -70 mV and did not exhibit voltage-dependent currents (up to +200 mV in the absence or presence of AITC), thus preventing further evaluation (data not shown). In the distal portion of the C-terminus, a significant reduction in responsiveness to AITC was produced by mutations at the residue K1009 positioned between helices H2 and H3, at K1092, located in the predicted region of the α-helix H5, and at the residue R1099 between helices H5 and H6.

The phenotypes of AITC-induced activation of the helix H1 mutants K969A (Figure 2Ba) and K969I (Figure 2Bb) clearly differed from K969E (Figure 2Bc) and from wild-type channels (Figure 2A) in that their responses were smaller and the onset of the secondary phase (if any) was apparently slower. The K969E mutant did not exhibit significant changes in the average amplitude of the AITC-induced currents. In contrast to the wild type, however, it lacked the first, gradually increasing activation phase (Figure 2Bc), indicating that either the gating properties of the channel are altered or permeating Ca^{2+} contributes much faster or more effectively to the potentiation of the response. In helix H1 mutants K989E (Figure 2Bg) and K989N (Figure 2Bh), the steep secondary phase only developed upon prolonged (> 40 s) application. In K969R (Figure 2Bd), R975A (Figure 2Be), K989A (Figure 2Bf), K1071A (Figure 2Bk), and K1092A (Figure 2Bl), the secondary phase of activation was not observed within the ~40 s period of AITC exposure; the responses were small and tended to inactivate upon prolonged AITC stimulation. Notably, R975A exhibited only small, linearly increasing inward currents accompanied by marked increases in current noise, indicating that the AITC-evoked currents arose from a fast opening of ion channels. Mutations R975E and

R975W did not produce measurable currents in response to AITC at a holding potential of -70 mV and did not exhibit voltage-dependent currents up to +200 mV (data not shown). Thus in this initial screening we identified ten basic residues that when mutated disrupted channel sensitivity to AITC, indicating that the C-terminus is a critical modulatory domain of TRPA1.

Mapping residues critical for the regulation of TRPA1 by voltage

The voltage-dependent activation properties were assessed in another set of experiments from the steady-state conductances at various test potentials using a voltage step protocol from -80 mV up to +200 mV in steps of +20 mV, measured first in the extracellular control solution, and, in those mutants with altered AITC or voltage sensitivity, also in the maintained presence of 200 µM AITC. In these experiments, we took care to fully activate the channels and thus the voltage step protocol was applied immediately at the peak amplitude of the first AITC response (Figure 3A). By measuring the maximum steady-state outward currents at +200 mV recorded in extracellular control solution, we detected significant changes in eight alanine mutants at the 0.01 probability level (Figure 3B). Of these, K969 (Figure 3Ab-e), R975 (Figure 3Af), and K989 (Figure 3Ah-j) appeared to be of major importance for the voltage-dependent activation of TRPA1, since mutations at these sites exhibited phenotypes that were kinetically clearly different from the wild-type. The voltage-induced currents mediated by K1009A and K1071A, although significantly smaller in amplitude, were kinetically indistinguishable from the wild-type channel. In contrast, the outward currents mediated through R1099A were larger than those in wild-type TRPA1 (data not shown).

The charge-reversing mutation K969E (Figure 3C and 3D) had strong effects on three important parameters of voltage-dependent gating: (1) saturation followed by a decrease in the maximum outward conductance at voltages higher than about +140 mV, (2) increasing the current variance at strongly (> +100 mV) depolarizing potentials and (3) slowing the decay kinetics of tail currents that arise upon repolarization to –70 mV from various test potentials. This phenotype was particularly remarkable, because a similar pattern of responses at positive potentials was previously reported for wild-type mouse TRPA1 [18,28](see Discussion).

Under control conditions, mutations R975A, K989A, K989E exhibited higher outward current amplitudes (Figure 3B) and a stronger outward rectification than wild-type TRPA1 (rectification ratios $G_{+180\ mV}/G_{-60\ mV}$; 37.5 ± 2.2 for R975A, 18.8 ± 2.8 for K989A, and 28 ± 13 for K989E versus 11.1 ± 3.5 for wild-type; n = 3-6) (Figure 4A and 4B). Kinetically clearly different phenotypes were obtained with R975A, K988A, K989A, K989E, and K989N, which exhibited prominent changes in the onset kinetics of their voltage-induced responses (Figure 3Af-j). Specifically, in R975A (Figure 3Af), the onset of the voltage-induced outward currents was instantaneous upon depolarization and only very small tail currents were inwardly directed upon repolarization from +200 mV to –70 mV, indicating that the mutant has a very fast gating kinetics or that the inward movement of cations through the conduction pathway of the channel is blocked at negative membrane potentials. Compared to wild-type TRPA1 (53.1 ± 4.6 ms; n = 5), the activation time constant for outward currents measured at +200 mV, obtained by fitting a monoexponential function to the current traces (τ_{on}), was much faster in K988A (23.5 ± 2.2 ms; n = 4). Also, in K989A, τ_{on} was 25.9 ± 4.2 ms (n = 3) and this value was not significantly different from that in K989E (25.1 ± 3.6 ms; n = 5; P = 0.884) or K989N (32.7 ± 0.4 ms; n = 3; P = 0.49), implying that the functional changes

caused by mutations at position K989 are likely to be steric rather than affected by charge. In control extracellular solution (Figure 4Da and 4Db), the open probabilities for wild-type TRPA1 were apparently below 0.5 so that values for the voltage for half-maximal activation (V_{50}) could not be derived from steady-state currents [4,29]. In contrast, the conductance-to-voltage (*G-V)* relationships were shifted toward less depolarizing potentials in K969A (V_{50} = 107.2 ± 7.5 mV; n = 4), R975A (106 ± 14 mV; n = 7), and K989A (87.2 ± 16 mV; n = 3), indicating an enhanced voltage-dependent activity at more physiological potentials.

Conductance-to-voltage relationships obtained in the presence of AITC

Voltage is a weak partial activator of TRPA1 that synergizes with other stimuli such as AITC or Ca^{2+} and regulates channel opening in an allosteric manner [4,11,23,29]. To further characterize the sensitivity of voltage-induced activation for all mutants with altered phenotypes, we measured the voltage-dependent component of gating from the conductance-to-voltage (*G-V)* relationships obtained in the presence of 200 µM AITC, compared at positive versus negative membrane potentials (G_{+180}/G_{-60mV}). The *G-V* relationships were virtually voltage-independent in wild-type TRPA1 (1.3 ± 0,16; n = 6) and in K988A (1.1 ± 0.1; n = 3; Figure 4C, Figure 4Dc and 4Dd). In contrast, the percentage of the voltage-dependent component of AITC-induced gating (G_{+180}/G_{-60mV}) was strongly ($P < 0.01$) increased in R975A (3.40 ± 0.68; n = 3), K989A (7.7 ± 2.0; n = 3), K989E (8.6 ± 2.0; n = 6) and K989N (3.45 ± 0.47; n = 6)(Figure 4B and C, Figure 4Dc and 4Dd). Similarly to what was observed in control extracellular solution (Figure 3D), K969E exhibited saturation followed by a decrease in the maximum outward conductance at voltages higher than about +120-140 mV (Figure 4Dd), which might indicate that the negative charge at this position interferes with the outward permeation of cations or that the mutation caused a defect in the voltage-dependent gating (see Discussion for additional possibilities).

Taken together, this data points to a possible differential role for K969, R975, K988, K989, and K1009, K1071 and R1099 in the voltage-dependent modulation of TRPA1. Except for K988, mutations at these residues also altered the AITC sensitivity (Figure 2C). Moreover, the potentiating effects of mutations at K989 were independent of the charge, suggesting that they might arise from the removal of the long lysine side chain. Thus, the changes in voltage-dependent activation in this mutant are probably due to alterations in channel gating rather than a direct effect on the putative voltage-transduction mechanism.

DISCUSSION

In this study, by performing the systemic neutralization of 27 positively charged residues within the C-terminal region of human TRPA1, we identified a limited number of residues that appear to be important to the allosteric regulation of the channel by both chemical and voltage stimuli (K969, R975, K989, K1009, K1046, K1071, K1092 and R1099). These residues are therefore most likely involved in the transduction of the activation signals to the gate rather than being the primary sites for either AITC binding or voltage sensing. In addition, we characterized three charge-neutralizing 'gain-of-function' mutants (R975A, K988A, and K989A) which exhibited higher sensitivity to depolarizing voltages, indicating that these residues may be directly involved in the voltage-dependent modulation of TRPA1.

Functional role of the most proximal helix of the C-terminus

Site directed mutagenesis studies have previously shown that AITC activates TRPA1 by covalently reacting with cysteine residues in the cytoplasmic N terminus of the channel [4,5]. The C-terminal basic residues, mutations of which significantly reduced responsiveness to AITC, thus may be part of a transduction region which transmits AITC signal from the N terminus to the gate. Those residues that are structurally proximal to the sixth transmembrane domain may directly participate in channel gating or contribute to the formation of permeation pathway. Also, the possibility of indirect electrostatic effects (such as interaction with some negatively charged ligands) cannot be excluded for any of the affected residues.

Mutation of K969 to glutamate produced a channel with a very distinctive phenotype: This mutant did not exhibit significant changes in the average amplitude of the AITC-induced currents but it lacked the first, gradually increasing activation phase (Figure 2Bc and Supplementary Figure S1A). This might indicate that either the gating properties of the channel are altered and/or permeating Ca^{2+} contributes much faster or more effectively to the potentiation of the responses. In order to further distinguish if the mutation-induced changes in the functionality of K969E stem from changes in gating or from alterations in the ion permeation or selectivity properties, we measured the Ca^{2+} permeability relative to Cs^{+} (Supplementary Figure S1B). We found that the K969E mutation yielded channels with unchanged permeability to Ca^{2+} ($P_{Ca}/P_{Cs} = 3.0 \pm 0.2$; $n = 7$, versus 3.4 ± 0.3 for wild-type; $n = 6$; $P < 0.05$) which indicates that the K969E mutation does not affect the ion permeation process and most likely does not indirectly influence Ca^{2+}-dependent gating at negative membrane potentials. Such a conclusion is further strengthened by our previously reported data showing that E966, which is located approximately one helix turn downward from K969, is probably poorly situated within the transmembrane electric field and neither sterically nor electrostatically contributes to forming the ion conduction pathway [27]. The charge-reversing mutation K969E had strong effects on voltage-dependent activation: at depolarizing potentials higher than about +140 mV, the maximum outward currents were decreased, whereas the current variance increased (Figure 3C and 3D). In addition, various mutations at K969 revealed that the channel does not well tolerate alanine, isoleucine or arginine at this position, which might be an additional indication that K969 indeed plays a structural role in gating. Interestingly, a similar pattern of decay of responses at positive membrane potentials was previously reported for CHO cells expressing wild-type mouse TRPA1 and has been attributed to channel inactivation [18] or to ‘a time-dependent increase in open probability, overlaid by a block of the ion channels by some unknown mechanism’ [28]. Moreover, in the latter study, very similar voltage-dependent properties were seen with H_2O_2 and AITC-evoked currents in calcium-free solution, indicating that Ca^{2+}-dependent inactivation of TRPA1 is not the likely mechanism.

Possible involvement of C-terminus in voltage-dependent activation

Mutations at R975, K988 and K989 directly affected voltage-dependent gating under control conditions, suggesting that these residues may be part of a voltage sensor. In contrast to voltage gated potassium channels, the voltage sensitivity of TRPA1 is very weak and there is virtually nothing known about what parts of the channel are involved in voltage sensing [30].

Therefore, it is not clear whether these three residues might be included in the electric field of the membrane. The robust steady-state outward rectification and leftward shift in the voltage-dependent activation observed in R975A and K989A (and, to a lesser extent, also in K988A) may be the consequence of the fact that both residues are situated on the same (more hydrophobic) side of the first proximal helix: the neutralization of either of these residues could similarly reduce the overall electrostatic effect.

The saturating concentration of agonist has been shown to reveal the voltage-independent component of gating in TRPA1-related TRPV1 and TRPM8 channels [31]. By using a voltage stimulus in combination with a supramaximal concentration of AITC (200 μM), we hoped to distinguish between the voltage-dependent and voltage-independent modes of TRPA1 activation to better understand the specific role of the identified residues. In thermosensitive TRP channels, chemical and thermal stimuli interact allosterically through independent molecular mechanisms. In TRPV1, vanilloids interact at intracellular/intramembranous regions in and adjacent to S3 and S4 [32,33]; a small region of the proximal part of the C-terminal domain renders the TRPV1 channel heat-sensitive and this region is transplantable into the cold-sensitive TRPM8 channel, whose voltage-induced responses become potentiated by heat [34]. A strong piece of evidence in favor of mechanistically distinguishable activation mechanisms was also recently presented for TRPV1 and TRPV3, in which agonist- and temperature-induced activations are separable from other activation mechanisms [35-38]. However, the intrinsic mechanism by which polymodal TRP channels are gated by voltage is much less clear. In another TRPA1-related channel, TRPV4, the main agonist-activated intracellular gate works independently of the voltage-dependent gating mechanism [39]. As pointed out by the authors (see Discussion in [39]), several possible candidates for the voltage gating mechanism have to be generally considered for the family of TRP-related cation channels: One of the possible models relies on a filter gating mechanism, which is based on the recently published evidence that filter region gating underlies TRPV1-channel activation [40,41]. In this case, the principle role for voltage might be the control of the direction of the driving force. This seems unlikely in TRPA1 because the channel becomes voltage-independent in the presence of a supersaturating concentration of AITC (Figure 4D). Another model of the voltage-dependent gating mechanism relies on direct voltage-dependent closure of the intracellular gate. Given that the activation rates upon depolarization were substantially accelerated in R975A, K988A, and K989A, we cannot dismiss the possibility that these residues could be directly involved in the voltage-dependent gating.

CONCLUSIONS

In this study, we identified the residues within the putative C-terminal tail of the human TRPA1 channel that when mutated affect its AITC and/or voltage sensitivity. In most cases, the reduced magnitudes of the responses to AITC or voltage were not due to reduced expression levels or plasma membrane targeting, since a) simultaneous application of both stimuli revealed considerable differences in the relative cross-sensitization capacity among the mutants, b) several mutants were less specifically responsive to AITC or voltage, i.e., their current-voltage relationships were qualitatively different from that in the wild-type channel or their AITC-induced inward currents lacked the steep secondary phase of activation, and, moreover, c) although there was a substantial overlap between the AITC- and voltage-deficient mutants, several of them exhibited significantly opposite effects on these two modalities (e.g. R975A, R989A, R1099A; compare Figure 2C with Figure 3B). Although

further mutagenesis is required to determine the exact nature of the identified residues, our findings provide strong support for the role of multiple basic residues in the recognition of chemical and voltage stimuli and indicate that the C-terminus is a critical modulatory domain for TRPA1 activation.

FUNDING

This work was supported by the Czech Science Foundation [305/06/0319, 301/10/1159], the Research Project Fund of the AS CR [AV0Z50110509, AV0Z60870520, IAA 600110701], and by the Ministry of Education, Youth and Sports of the Czech Republic [1M0517, LC06010, MSM6007665808 and LC554].

REFERENCES

1 Story, G. M., Peier, A. M., Reeve, A. J., Eid, S. R., Mosbacher, J., Hricik, T. R., Earley, T. J., Hergarden, A. C., Andersson, D. A., Hwang, S. W., McIntyre, P., Jegla, T., Bevan, S. and Patapoutian, A. (2003) ANKTM1, a TRP-like channel expressed in nociceptive neurons, is activated by cold temperatures. Cell **112**, 819-829

2 Zhang, X. F., Chen, J., Faltynek, C. R., Moreland, R. B. and Neelands, T. R. (2008) Transient receptor potential A1 mediates an osmotically activated ion channel. Eur. J. Neurosci. **27**, 605-611

3 Sawada, Y., Hosokawa, H., Hori, A., Matsumura, K. and Kobayashi, S. (2007) Cold sensitivity of recombinant TRPA1 channels. Brain Res. **1160**, 39-46

4 Macpherson, L. J., Dubin, A. E., Evans, M. J., Marr, F., Schultz, P. G., Cravatt, B. F. and Patapoutian, A. (2007) Noxious compounds activate TRPA1 ion channels through covalent modification of cysteines. Nature **445**, 541-545

5 Hinman, A., Chuang, H. H., Bautista, D. M. and Julius, D. (2006) TRP channel activation by reversible covalent modification. Proc. Natl. Acad. Sci. U. S. A. **103**, 19564-19568

6 Cavanaugh, E. J., Simkin, D. and Kim, D. (2008) Activation of transient receptor potential A1 channels by mustard oil, tetrahydrocannabinol and Ca(2+) reveals different functional channel states. Neuroscience **154**, 1467-1476

7 Garcia-Anoveros, J. and Nagata, K. (2007) TRPA1. Handb. Exp. Pharmacol., 347-362

8 Bautista, D. M., Jordt, S. E., Nikai, T., Tsuruda, P. R., Read, A. J., Poblete, J., Yamoah, E. N., Basbaum, A. I. and Julius, D. (2006) TRPA1 mediates the inflammatory actions of environmental irritants and proalgesic agents. Cell **124**, 1269-1282

9 Nagata, K., Duggan, A., Kumar, G. and Garcia-Anoveros, J. (2005) Nociceptor and hair cell transducer properties of TRPA1, a channel for pain and hearing. J. Neurosci. **25**, 4052-4061

10 Doerner, J. F., Gisselmann, G., Hatt, H. and Wetzel, C. H. (2007) Transient receptor potential channel A1 is directly gated by calcium ions. J. Biol. Chem. **282**, 13180-13189

11 Zurborg, S., Yurgionas, B., Jira, J. A., Caspani, O. and Heppenstall, P. A. (2007) Direct activation of the ion channel TRPA1 by Ca2+. Nat. Neurosci. **10**, 277-279

12 Wang, Y. Y., Chang, R. B., Waters, H. N., McKemy, D. D. and Liman, E. R. (2008) The Nociceptor Ion Channel TRPA1 Is Potentiated and Inactivated by Permeating Calcium Ions. J. Biol. Chem. **283**, 32691-32703

13 Bandell, M., Story, G. M., Hwang, S. W., Viswanath, V., Eid, S. R., Petrus, M. J., Earley, T. J. and Patapoutian, A. (2004) Noxious cold ion channel TRPA1 is activated by pungent compounds and bradykinin. Neuron **41**, 849-857

14 Wang, S., Dai, Y., Fukuoka, T., Yamanaka, H., Kobayashi, K., Obata, K., Cui, X., Tominaga, M. and Noguchi, K. (2008) Phospholipase C and protein kinase A mediate bradykinin sensitization of TRPA1: a molecular mechanism of inflammatory pain. Brain **131**, 1241-1251

15 Nilius, B., Owsianik, G. and Voets, T. (2008) Transient receptor potential channels meet phosphoinositides. EMBO J. **27**, 2809-2816

16 Corey, D. P., Garcia-Anoveros, J., Holt, J. R., Kwan, K. Y., Lin, S. Y., Vollrath, M. A., Amalfitano, A., Cheung, E. L., Derfler, B. H., Duggan, A., Geleoc, G. S., Gray, P. A., Hoffman, M. P., Rehm, H. L., Tamasauskas, D. and Zhang, D. S. (2004) TRPA1 is a candidate for the mechanosensitive transduction channel of vertebrate hair cells. Nature **432**, 723-730

17 Hirono, M., Denis, C. S., Richardson, G. P. and Gillespie, P. G. (2004) Hair cells require phosphatidylinositol 4,5-bisphosphate for mechanical transduction and adaptation. Neuron **44**, 309-320

18 Karashima, Y., Prenen, J., Meseguer, V., Owsianik, G., Voets, T. and Nilius, B. (2008) Modulation of the transient receptor potential channel TRPA1 by phosphatidylinositol 4,5-biphosphate manipulators. Pflugers Arch.

19 Akopian, A. N., Ruparel, N. B., Jeske, N. A. and Hargreaves, K. M. (2007) Transient receptor potential TRPA1 channel desensitization in sensory neurons is agonist dependent and regulated by TRPV1-directed internalization. J. Physiol. **583**, 175-193

20 Kim, D., Cavanaugh, E. and Simkin, D. (2008) Inhibition of Transient Receptor Potential A1 by Phosphatidylinositol-4,5-bisphosphate. Am J Physiol Cell Physiol

21 Rohacs, T. (2009) Phosphoinositide regulation of non-canonical transient receptor potential channels. Cell Calcium **45**, 554-565

22 Suh, B. C. and Hille, B. (2008) PIP2 is a necessary cofactor for ion channel function: how and why? Annu Rev Biophys **37**, 175-195

23 Karashima, Y., Talavera, K., Everaerts, W., Janssens, A., Kwan, K. Y., Vennekens, R., Nilius, B. and Voets, T. (2009) TRPA1 acts as a cold sensor in vitro and in vivo. Proc. Natl. Acad. Sci. U. S. A. **106**, 1273-1278

24 Susankova, K., Ettrich, R., Vyklicky, L., Teisinger, J. and Vlachova, V. (2007) Contribution of the putative inner-pore region to the gating of the transient receptor potential vanilloid subtype 1 channel (TRPV1). J. Neurosci. **27**, 7578-7585

25 Vlachova, V., Teisinger, J., Sušánková, K., Lyfenko, A., Ettrich, R. and Vyklicky, L. (2003) Functional role of C-terminal cytoplasmic tail of rat vanilloid receptor 1. J. Neurosci. **23**, 1340-1350

26 Dittert, I., Benedikt, J., Vyklicky, L., Zimmermann, K., Reeh, P. W. and Vlachova, V. (2006) Improved superfusion technique for rapid cooling or heating of cultured cells under patch-clamp conditions. J. Neurosci. Methods **151**, 178-185

27 Benedikt, J., Samad, A., Ettrich, R., Teisinger, J. and Vlachova, V. (2009) Essential role for the putative S6 inner pore region in the activation gating of the human TRPA1 channel. Biochim. Biophys. Acta Mol. Cell. Research **1793**, 1279-1288

28 Andersson, D. A., Gentry, C., Moss, S. and Bevan, S. (2008) Transient receptor potential A1 is a sensory receptor for multiple products of oxidative stress. J. Neurosci. **28**, 2485-2494

29 Karashima, Y., Damann, N., Prenen, J., Talavera, K., Segal, A., Voets, T. and Nilius, B. (2007) Bimodal action of menthol on the transient receptor potential channel TRPA1. J. Neurosci. **27**, 9874-9884

30 Latorre, R., Zaelzer, C. and Brauchi, S. (2009) Structure-functional intimacies of transient receptor potential channels. Q. Rev. Biophys. **42**, 201-246

31 Matta, J. A. and Ahern, G. P. (2007) Voltage is a partial activator of rat thermosensitive TRP channels. J. Physiol. **585**, 469-482

32 Jordt, S. E. and Julius, D. (2002) Molecular basis for species-specific sensitivity to "hot" chili peppers. Cell **108**, 421-430.

33 Gavva, N. R., Klionsky, L., Qu, Y., Shi, L., Tamir, R., Edenson, S., Zhang, T. J., Viswanadhan, V. N., Toth, A., Pearce, L. V., Vanderah, T. W., Porreca, F., Blumberg, P. M., Lile, J., Sun, Y., Wild, K., Louis, J. C. and Treanor, J. J. (2004) Molecular determinants of vanilloid sensitivity in TRPV1. J. Biol. Chem. **279**, 20283-20295

34 Brauchi, S., Orta, G., Mascayano, C., Salazar, M., Raddatz, N., Urbina, H., Rosenmann, E., Gonzalez-Nilo, F. and Latorre, R. (2007) Dissection of the components for PIP2 activation and thermosensation in TRP channels. Proc. Natl. Acad. Sci. U. S. A. **104**, 10246-10251

35 Hu, H., Grandl, J., Bandell, M., Petrus, M. and Patapoutian, A. (2009) Two amino acid residues determine 2-APB sensitivity of the ion channels TRPV3 and TRPV4. Proc. Natl. Acad. Sci. U. S. A. **106**, 1626-1631

36 Grandl, J., Hu, H., Bandell, M., Bursulaya, B., Schmidt, M., Petrus, M. and Patapoutian, A. (2008) Pore region of TRPV3 ion channel is specifically required for heat activation. Nat. Neurosci. **11**, 1007-1013

37 Yang, F., Cui, Y., Wang, K. and Zheng, J. (2010) Thermosensitive TRP channel pore turret is part of the temperature activation pathway. Proc. Natl. Acad. Sci. U. S. A.

38 Grandl, J., Kim, S. E., Uzzell, V., Bursulaya, B., Petrus, M., Bandell, M. and Patapoutian, A. (2010) Temperature-induced opening of TRPV1 ion channel is stabilized by the pore domain. Nat. Neurosci.

39 Loukin, S., Su, Z., Zhou, X. and Kung, C. (2010) Forward-genetic analysis reveals multiple gating mechanisms of Trpv4. J. Biol. Chem.

40 Myers, B. R., Bohlen, C. J. and Julius, D. (2008) A yeast genetic screen reveals a critical role for the pore helix domain in TRP channel gating. Neuron **58**, 362-373

41 Ryu, S., Liu, B., Yao, J., Fu, Q. and Qin, F. (2007) Uncoupling proton activation of vanilloid receptor TRPV1. J. Neurosci. **27**, 12797-12807

Figure Legends

Figure 1

Scanning mutagenesis of C-terminus of human TRPA1 channel. (**A**) Putative secondary structure of hTRPA1 channel subunit with six transmembrane domains and single-letter coded amino acid sequence of C-terminus. α-helices are shown as cylinders. Positively charged amino acids are indicated. The residues, mutations of which were found to affect the function of TRPA1, are indicated by bold white letters on black squares. (**B**) Sequence comparison of C-terminus of human TRPA1 (GeneBank accession number NM_007332) with that of mouse mTRPA1 (NM_177781) and rat rTRPA1 (NM_207608). Secondary structure was determined using consensus of four prediction servers (PredictProtein, jPRED, APSSP2, YASSPP). The structure was assigned if at least 3 of 4 servers predict to the residuum the same structure with an expected average accuracy over 80% or reliability over 5. Based on these conditions, the C-terminus is predicted to contain two long and four short helices: I964-K989 (H1), W993-V998 (H2), L1016-F1022 (H3), L1040-K1071 (H4), D1089-Q1095 (H5), W1103-K1111 (H6).

Figure 2

Screen of C-terminus of hTRPA1 for AITC sensitivity. (**A**) Examples of whole-cell currents elicited by 200 μM AITC from HEK293T cells transiently transfected with wild-type TRPA1 or (**B, a-m**) mutant TRPA1 channels that exhibited the most prominent phenotypic changes. Dashed lines indicate zero current level. Horizontal bars above each record indicate the duration of AITC application. Holding potential -70 mV. (**C**) Summary of scanning mutagenesis results comparing sensitivity to AITC. The right bar graph shows mean whole-cell currents evoked by 200 μM AITC at –70 mV measured at the peak for each construct. Each bar is the mean ± SEM of at least six independent cells. The left bar graph represents the probabilities obtained from the *t*-tests that were performed in order to determine if there is a significant difference between the responses of the wild-type and the individual mutants. Statistical significance ($P < 0.01$) is indicated with asterisks in the right current bar chart. The plus signs indicate positions where mutations resulted in constructs lacking functional expression in HEK293T cells. The level of significance is indicated with a dashed vertical line in the left probability bar graph. The predicted secondary structure is indicated in the middle as vertical thick bars (α-helices H1, H2, H4-H6).

Figure 3

Voltage-dependent gating of TRPA1 mutants. (**A**) Representative current traces in response to indicated voltage step protocol (holding potential, -70 mV; voltage steps from -80 mV to +200 mV; increment, +20 mV) recorded in control extracellular solution (left) and in the presence of 200 μM AITC (right). (**B**) Summary of mutagenesis results. Average

steady-state whole-cell currents induced by voltage (+200 mV). Each bar is the mean ± SEM of at least six independent cells. The predicted secondary structure is indicated in the middle as vertical thick bars (α-helices H1, H2, H4-H6). The left bar graph represents the probabilities obtained from the *t*-tests that compared the steady-state current amplitudes of the individual mutants with the wild-type. Statistical significance ($P < 0.01$) is indicated with asterisks in the right current bar chart. The level of significance is indicated with a dashed vertical line in the left probability bar graph. (**C**) Representative whole-cell currents evoked by voltage protocol (shown in A) applied in control extracellular solution, recorded in K969E mutant. (**D**) Averaged voltage-current relationship constructed from responses obtained from 8 independent recordings such as shown in C, measured at the end of the pulses (indicated above the records in C). Data is means ± SEM.

Figure 4

Effects of mutations on the AITC-modulation of voltage-dependent gating. (**A**) Effects of 200 μM AITC on maximal voltage-induced outward currents of TRPA1 mutants. Steady-state currents evoked by +200 mV measured in the absence (open bars) and presence of 200 μM AITC (filled bars). (**B**) Outward rectification properties (G_{+180mV}/G_{-60mV}) reflecting the effects of mutations on voltage-dependent gating. (**C**) Summary of voltage-dependent component of AITC-induced gating (G_{+180mV}/G_{-60mV}). Asterisks indicate significance level ($P < 0.01$). (**D**) Summary of whole-cell conductances obtained in the absence (left graphs) and presence of 200 μM AITC (right graphs) for wild-type and for indicated constructs. Under control conditions, the wild-type channels and some mutants did not reach half-maximal activation at voltages up to +200 mV. Each plot is the mean ± SEM; $n = 3$-8.

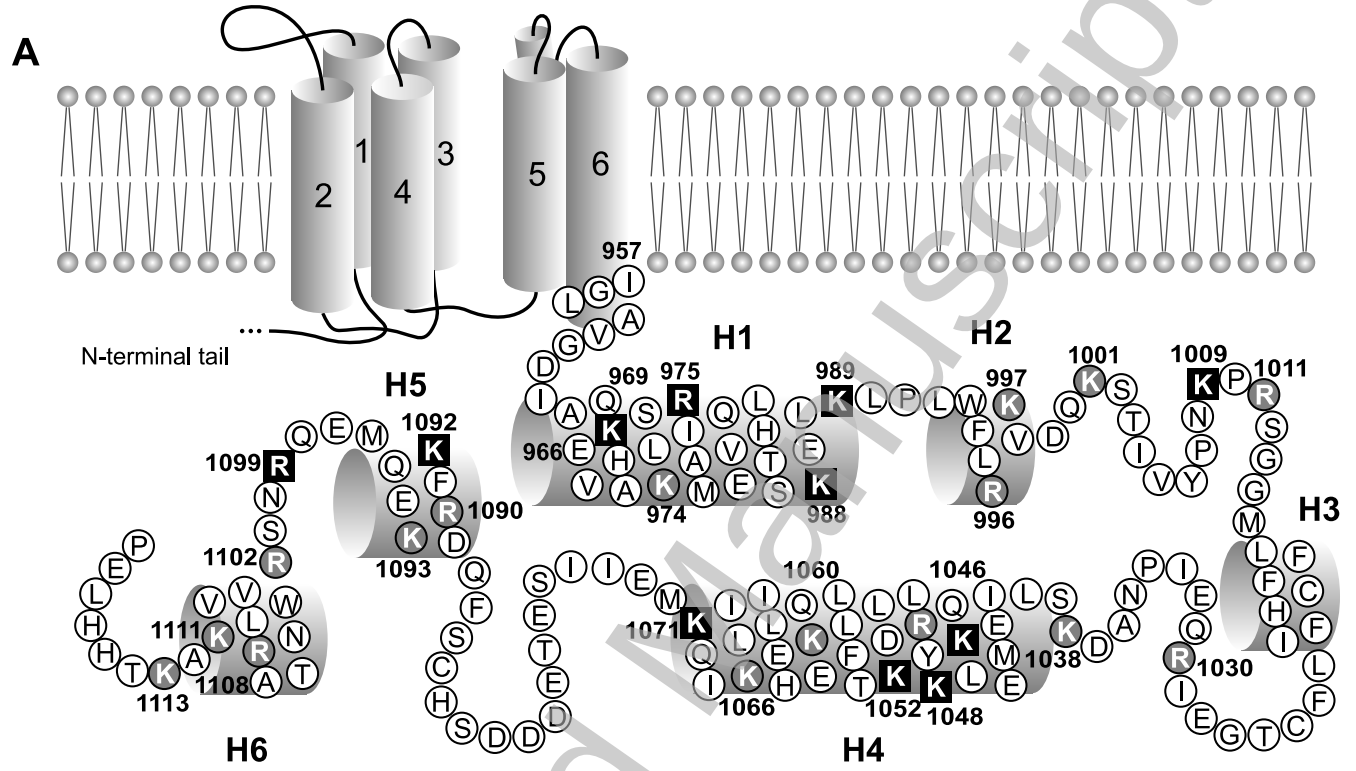

B

```
          960       970       980       990       1000      1010      1020      1030
hTRPA1 GLAVGDIAEVQKHASLKRIAMQVELHTSLEKKLPLWFLRKVDQKSTIVYPNKPRSGGMLFHIFCFLFCTGEIRQEIPNADKS
mTRPA1 GLAVGDIAEVQKHASLKRIAMQVELHTNLEKKLPLWYLRKVDQRSTIVYPNRPRHGRMLR~FFHYFLNMQETRQEVPNIDTC
rTRPA1 GLAVGDIAEVQKHASLKRIAMQVELHTNLEKKLPFWYLRKVDQRSTIVYPNRPRHGRMLR~FFHYFLSMQETRQEAPNIDTC
       ****************************.******:*:******:*******:** * **  :* :::   * *** ** *..

          1040      1050      1060      1070      1080      1090      1100      1110
hTRPA1 LEMEILKQKYRLKDLTFLLEKQHELIKLIIQKMEIISETEDDDSHCSFQDRFKKEQMEQRNSRWNTVLRAVKAKTHHLEP~~~~
mTRPA1 LEMEILKQKYRLKDLTSLLEKQHELIKLIIQKMEIISETEDEDNHCSFQDRFKKERLEQMHSKWNFVLNAVKTKTHCSISHPDF
rTRPA1 LEMEILKQKYRLKDLTSLLEKQHELIKLIIQKMEIISETEDEDNHCSFQDRFKKERLEQMHSKWNFVLNAVKTKTHCSISHPDI
       **************** ************************:*.**********::** :*:** **.***:***    .
```

Figure 1

Biochemical Journal Immediate Publication. Published on 14 Oct 2010 as manuscript BJ20101256

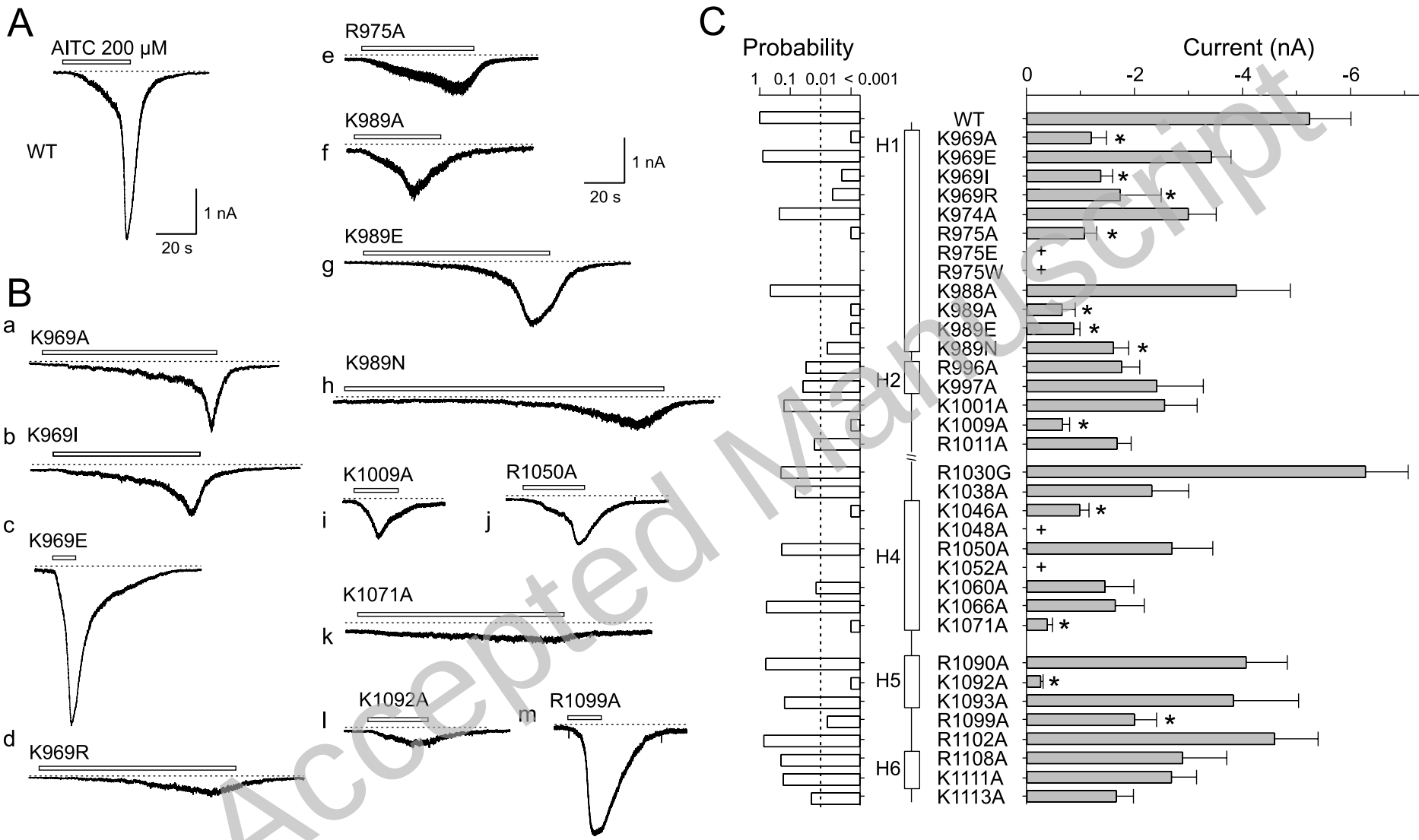

Figure 2

Biochemical Journal Immediate Publication. Published on 14 Oct 2010 as manuscript BJ20101256

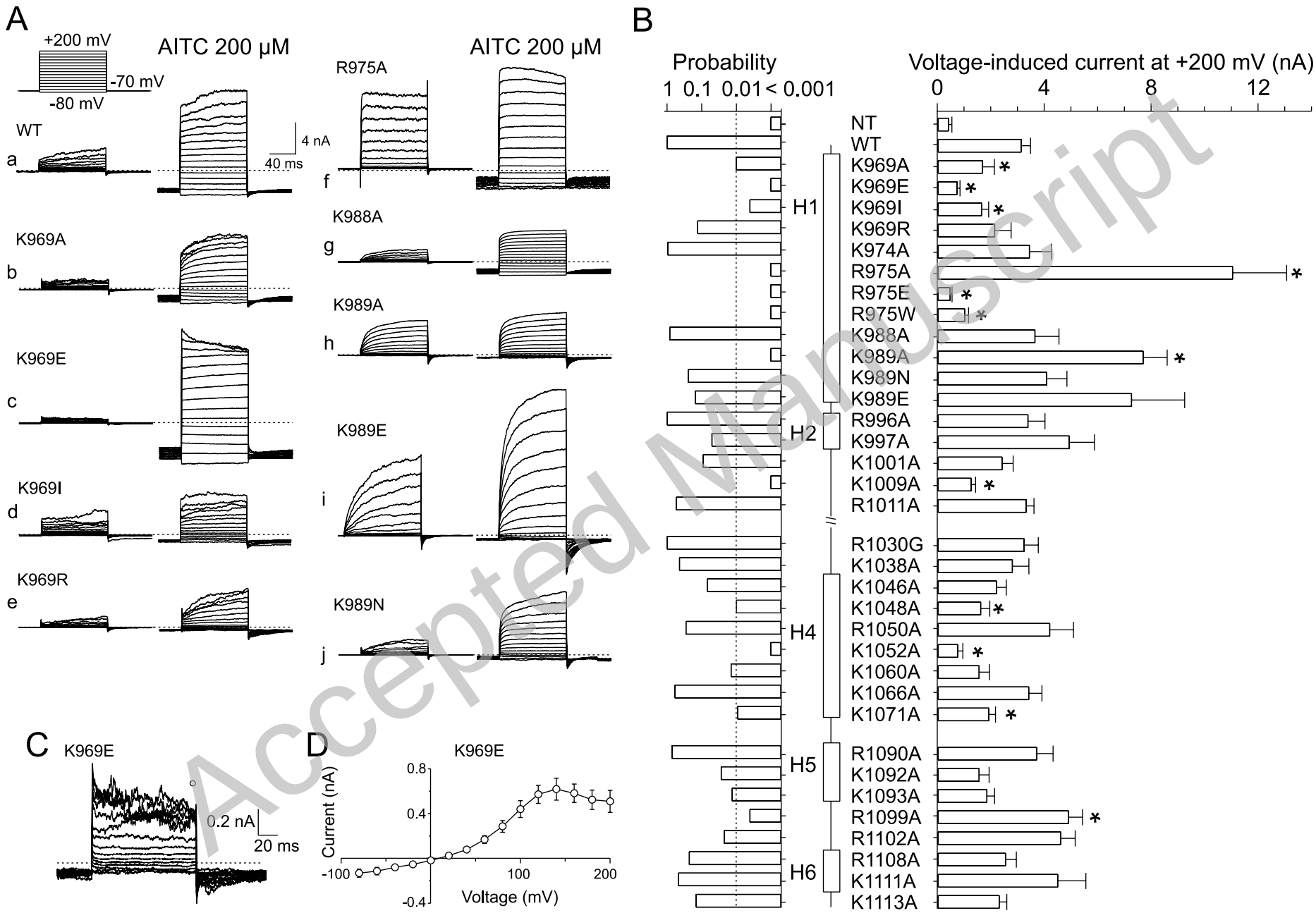

Figure 3

Biochemical Journal Immediate Publication. Published on 14 Oct 2010 as manuscript BJ20101256

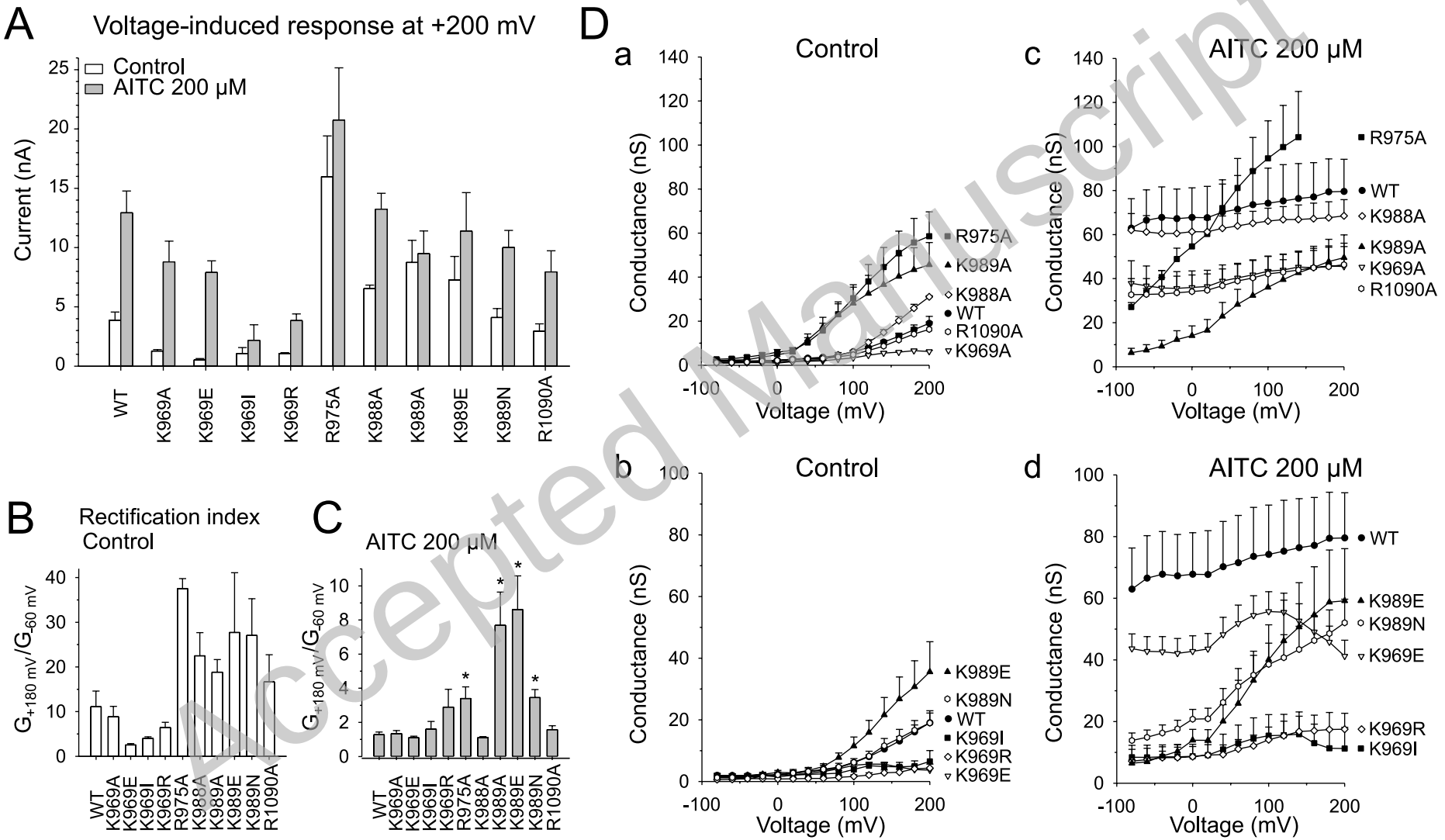

Figure 4